Reprinted from

ATMOSPHERIC RESEARCH

Atmospheric Research 36 (1995) 69–94

Theory of the water vapor continuum and validations

R.H. Tipping[a], Q. Ma[b]

[a]*Department of Physics and Astronomy, University of Alabama, Tuscaloosa, AL 35487, USA*
[b]*Department of Applied Physics, Columbia University, New York, NY, 10027, USA*

ELSEVIER

ATMOSPHERIC RESEARCH

Formerly: Journal de Recherches Atmosphériques

Scope of the journal. *Atmospheric Research* will publish scientific papers (research papers, review articles and notes) dealing with the part of the atmosphere where meteorological events occur. Attention will be given to all processes extending from the earth surface to the tropopause, but special emphasis will continue to be devoted to the physics of clouds and precipitation, i.e. atmospheric aerosols, microphysical processes, cloud dynamics and thermodynamics, numerical simulation of cloud processes, clouds and radiation, meso- and macrostructure of clouds and cloud systems, and weather modification.

0169-8095/95/$ 09.50

ELSEVIER

Atmospheric Research 36 (1995) 69–94

ATMOSPHERIC RESEARCH

Theory of the water vapor continuum and validations

R.H. Tipping[a], Q. Ma[b]

[a]*Department of Physics and Astronomy, University of Alabama, Tuscaloosa, AL 35487, USA*
[b]*Department of Applied Physics, Columbia University, New York, NY, 10027, USA*

Received 30 April, 1993; revised and accepted 11 March, 1994

Abstract

A far-wing line shape theory based on the binary collision and quasistatic approximations that is applicable for both the low- and high-frequency wings of the vibration-rotational bands has been developed. This theory has been applied in order to calculate the frequency and temperature dependence of the continuous absorption coefficient for frequencies up to 10,000 cm^{-1} for pure H_2O and for H_2O–N_2 mixtures. The calculations were made assuming an interaction potential consisting of an isotropic Lennard-Jones part with two parameters that are consistent with values obtained from other data, and the leading long-range anisotropic part, together with the measured line strengths and transition frequencies. The results, obtained without the introduction of adjustable parameters, compare well with the existing laboratory data, both in magnitude and in temperature dependence. This leads us to the conclusion that the water continuum can be explained in terms of far-wing absorption. Current work in progress to extend the theory and to validate the theoretically calculated continuum will be discussed briefly.

1. Introduction

The absorption of radiation by water vapor in the window regions of the Earth's atmosphere is a problem of great practical as well as theoretical interest (Deepak et al., 1980). In the past few years there have been a number of general reviews (Hinderling et al., 1987; Varanasi, 1988a; Grant, 1990; Thomas, 1990) concentrating primarily on the experimental characterization of this absorption; for historical reasons this absorption is called the "water continuum" and the interested reader is referred to these reviews for original literature citations. As a result of this extensive work, there is nearly unanimous agreement on the density depen-

0169-8095/95/$09.50
SSDI 0169-8095(94)00028-C

dence (quadratic), general agreement on the temperature dependence (strong, negative, at least in the 8–13 μm window for atmospheric temperatures), but considerable disagreement as to the magnitude and physical mechanism responsible for the absorption. Water dimers (Penner and Varanasi, 1967), polymers (Carlon, 1981), collision-induced absorption (Birnbaum, 1985), and the superposition of the far wings of collisionally broadened allowed dipole lines (Elsasser, 1938) have all been suggested as possible sources of the water continuum. While the first two mechanisms are undoubtedly present and contribute to the absorption in the atmosphere (in varying amounts in the different spectral regions), there is increasing evidence to believe that they are not the primary mechanism. Although collision-induced absorption arising from binary collisions between water molecules would have the correct quadratic density dependence and strong, negative temperature variation, its magnitude is too small to explain the observed absorption. The dimer model, on the other hand, has a temperature dependence similar to that observed near room temperature in the 8–13 μm window (Roberts et al., 1976; Varanasi, 1988a; Thomas, 1990). However, this predicted temperature dependence is not in agreement with that of the observed continuum in other spectral regions (Burch, 1982; Thomas, 1990). Furthermore, the density dependence in the wings of the bands (presumably responsible for the continuum absorption) would vary as the cube of the density in disagreement with the experimental results; also no spectral features unambiguously assigned to dimers have been identified in the laboratory data or in atmospheric measurements.

Within the past decade, substantial progress for calculating the absorption far from the line centers of resonant transitions has been made. Starting from the basic formalism of Davies et al. (1982), Rosenkranz (1985, 1987) has developed a quasistatic theory that is applicable in the high-frequency wing of the pure rotational band (the 8–13 μm window). This theory successfully predicted both the magnitude and the strong, negative temperature dependence. This theory was extended by Ma and Tipping (1990a), but, because of the nature of the approximations made, was limited to the high-frequency wings of the pure rotational and/or the vibrational bands. Utilizing the same basic formalism, but proceeding in a different way mathematically, these authors also developed a theory (Ma and Tipping, 1990b) that was applicable for the low-frequency wing of the pure rotational band, i.e., for the millimeter spectral region. Again, good agreement in both magnitude and temperature dependence between theory and experiment (Liebe, 1989) was obtained.

More recently, a new far-wing line shape theory based on the binary collision and quasistatic approximations was formulated (Ma and Tipping, 1991) and applied to calculate the absorption coefficient, $\alpha(\omega)$, for frequencies ω between 300 and 1100 cm^{-1} for several temperatures. The results were in excellent agreement with the extensive experimental data of Burch and co-workers (1984, 1985). In particular, by treating the resonant and anti-resonant terms separately, better agreement with the high-temperature laboratory data was obtained as compared to the theory of Rosenkranz (1985, 1987). This new theory has been generalized

to vibration-rotational bands (Ma and Tipping, 1992a) and to foreign broadening (Ma and Tipping, 1992b), and thus constitutes a unified theoretical framework within which one can calculate the magnitude and temperature dependence of the self and foreign broadened far-wing absorption.

Prior to the work of Rosenkranz (1985, 1987) and the development of the present theory, several previous attempts to model the continuum absorption in H_2O and H_2O–N_2 mixtures have been made. Roberts et al. (1976) derived an analytic expression for the continuum in the 8–13 μm region by fitting the data of Burch et al. (1971, 1974, 1975). This formulation is still widely used because of its simplicity, but it does not reproduce the improved experimental laboratory data of Burch and co-workers (1982, 1984, 1985), nor does it model correctly the temperature dependence observed by Montgomery (1978) and by Loper et al. (1983). Thomas and Nordstrom (1980, 1982a, b, 1985) sought to model the continuum absorption in terms of a modified line shape. They assumed a Lorentzian line shape near the line center matched to a statistical line shape in the far wings using a large number of adjustable parameters fit to various spectral regions at different temperatures. When extrapolated to other regions or to different temperatures, their results are not in agreement with experimental data. A more sophisticated line shape model was developed by Clough and co-workers (1980, 1983) who attempted to include as much physics as possible (fluctuation-dissipation theorem, Nyquist theorem, etc.) in their model. More recently, based on the early theoretical work of Davies et al. (1982), Clough et al. (1989) introduced an empirical line shape correction factor (χ function) that can be used to calculate the continuum contribution within the framework of FASCODE line-by-line calculations. This model, referred to as the CKD model, is based primarily on the data of Burch and co-workers, but over the years has been refined as a result of atmospheric comparisons. While it is certainly true that this approach is at present the best way to obtain the most accurate results over a wide range of frequencies without the introduction of a large number of ad hoc parameters, there are a number of drawbacks associated with this model. By introducing a single χ function that is symmetric in frequency displacement, the resulting absorption coefficient does not satisfy the principle of detailed balance (Ma and Tipping, 1994); this will not affect the results in the near-wing region, but can affect them in the far-wing region. The temperature dependence of the empirical χ function was obtained by fitting laboratory data at two temperatures (296 and 338 K); these results can be interpolated successfully in temperature over this narrow range, but the extrapolation to the much lower temperatures in the atmosphere can introduce additional uncertainties. In fact, there is some evidence (Kilsby et al., 1992) that the temperature dependence in the CKD model is responsible for the underestimate of the absorption in the 10–12 μm window by as much as 30% in a tropical atmosphere. Extrapolation of the model to high-temperature data can also lead to difficulties (Hartmann et al., 1993).

In the present paper, we do not make any attempt to compare the continuum models or the results obtained by the various authors mentioned above with our current results; neither do we compare our results with predictions made based

on alternative mechanisms (e.g., the dimer hypothesis). Rather, our purpose is to present the most recent theoretical results and to compare these with extensive experimental data in order to investigate whether far-wing absorption can account for the major features of the observed continuum absorption. Accordingly, the outline of the present paper is the following. In the next section, we first review the mathematical formalism and discuss the nature of the approximations made. In Section 3, we then discuss the computational details and present theoretical results for the positive and negative resonance theoretical line shapes and the resulting absorption coefficient $\alpha(\omega)$ up to 10,000 cm^{-1} for self and N_2 broadening. In Section 4, we compare our present theoretical results with selected experimental data. In this regard, it is important to keep in mind that we have not made any attempt to improve the agreement of our results with specific experimental data by adjusting the values of the input data. We also discuss briefly some preliminary validations of our theoretical results using atmospheric data, and conclude by mentioning some recent progress made to refine the present theory.

2. The general formalism

2.1. The absorption coefficient and spectral density

As is well known, if we divide a gaseous sample into an absorber molecule a and treat the remaining molecules as a bath, then the absorption of radiation of frequency ω (cm^{-1}) per unit volume of a sample in thermal equilibrium at temperature T is characterized by the absorption coefficient $\alpha(\omega)$:

$$\alpha(\omega)=\frac{4\pi^2}{3\hbar c}n_a\,\omega\tanh(\hbar\omega/2kT)\,[F(\omega)+F(-\omega)], \tag{1}$$

where c is the speed of light, n_a is the number density of absorbers and $F(\omega)$, the spectral density, is given by

$$F(\omega)=\frac{1}{\pi}Re\,Tr\int_0^\infty [\vec{\mu}_a\cdot e^{i(\omega-L)t}\rho\vec{\mu}_a]\,dt. \tag{2}$$

In this expression $\vec{\mu}_a$ is the dipole moment operator of the absorber molecule and L is the total Hermitian Liouville operator which can be expressed as the sum of its components

$$L=L_0+L_1=L^{(a)}+L^{(b)}+L_1.$$

We assume

$$e^{-iLt}\simeq e^{-iL_0t}e^{-iL_1t}. \tag{3}$$

Then Eq. (2) can be approximated by

$$F(\omega)=\frac{1}{\pi}Re\,Tr\int_0^\infty[\vec{\mu}_a\cdot e^{i(\omega-L_0)t}e^{-iL_1t}\rho\vec{\mu}_a]\mathrm{d}t. \tag{4}$$

By making a Laplace transformation of the operator $e^{-iL_1t}\rho\vec{\mu}_a$

$$e^{-iL_1t}\rho\vec{\mu}_a=\frac{1}{2\pi i}\int_{-\infty}^{\infty}e^{-i\omega' t}\frac{1}{\omega'-L_1}\rho\vec{\mu}_a\mathrm{d}\omega', \tag{5}$$

Eq. (4) can be rewritten as

$$F(\omega)=\frac{1}{\pi}\mathrm{Im}\frac{1}{2\pi i}\int_{-\infty}^{\infty}\mathrm{d}\omega' Tr[\vec{\mu}_a\cdot\frac{1}{\omega-\omega'-L_o}\times\frac{1}{\omega'-L_1}\rho\vec{\mu}_a]. \tag{6}$$

We assume that the total density operator can be approximated by the product of three parts

$$\rho=\rho^{(\mathrm{int})}\rho^{(\mathrm{b})}\rho^{(\mathrm{a})}, \tag{7}$$

where $\rho^{(\mathrm{a})}$ and $\rho^{(\mathrm{b})}$ are the parts related to the unperturbed absorber and bath molecules, respectively, and $\rho^{(\mathrm{int})}$ is the part related to the interaction between them. As a result we obtain an important expression for the spectral density in which formally all the variables except the internal variables of the absorber have been isolated

$$F(\omega)=\frac{1}{\pi}\mathrm{Im}\frac{1}{2\pi i}\int_{-\infty}^{\infty}\mathrm{d}\omega' Tr[\vec{\mu}_a\cdot\frac{1}{\omega-\omega'-L_a}\times <\frac{1}{\omega'-L_1}\rho^{(\mathrm{int})}>_b\rho^{(a)}\vec{\mu}_a]_a. \tag{8}$$

The Liouville operator $<(1)/(\omega'-L_1)\rho^{(\mathrm{int})}>_b$ contains all the information about the bath molecules and the interaction dynamics between the absorber molecule and the bath. Formally, this expression for the spectral density contains an integral. However, the integral does not complicate the calculations since it is easily carried out using the Cauchy integral formula.

Based on the binary collision approximation which is valid in the low-density limit, we can focus on the absorber molecule and one bath molecule. Then, in Eq. (8) and subsequent expressions, the Liouville operator L_1 and the summation index b are only related to these two molecules.

Since the isotropic interaction does not depend on the rotational quantum numbers, the Liouville operator associated with it will cancel out when it acts on the line space. Therefore, $V_{is}(r)$ need not be included in the interaction Liouville operator L_1. The Liouville operator corresponding to the anisotropic interaction between the absorber and the bath molecule is

$$L_1 = [V_{\text{anis}}(\vec{r})I^* - \mathrm{IV}^*_{\text{anis}}(\vec{r})]/\hbar$$
$$= (G_{\text{anis}}I^* - IG^*_{\text{anis}})/r^s, \tag{9}$$

where I ($=I^*$) is the identity operator and the exponent s is the power of the leading term in the expansion of the anisotropic interaction. For example, $s=3$ for the dipole–dipole interaction (H_2O–H_2O), $s=4$ for the dipole–quadrupole interaction (H_2O–N_2), etc. In the following, We denote by $|\alpha>$ and G_α, the eigenvectors and eigenvalues, respectively, of the matrix operator G_{anis}.

The resolvent operator $<(1)/(\omega' - L_1)\rho^{(\text{int})}>_b$ in Eq. (8) is an operator acting on the line space of the absorber molecule a. Therefore, in general, it can be expressed as

$$<\frac{1}{\omega - L_1}\rho^{(\text{int})}>_b = \sum_{i_1 j_1 i'_1 j'_1} <i_1 j_1{}^\dagger|$$
$$<\frac{1}{\omega - L_1}\rho^{(\text{int})}>_b |i'_1 j'^\dagger_1> |i_1 j^\dagger_1> <i'_1 j'^\dagger_1|, \tag{10}$$

where $|i_1 j^\dagger_1>$ are the basis in the line space of the absorber molecule, and i_1 stands for all quantum numbers specifying its states. By explicitly writing the summation over the internal variables of the bath molecule, its components can be written as

$$<i_1 j^\dagger_1| <\frac{1}{\omega - L_1}\rho^{(\text{int})}>_b |i'_1 j'^\dagger_1> = \sum_{i_2 j_2} \sum_{\alpha\beta} <i_1 i_2|\alpha><\beta|j_1 i_2$$
$$> Tr\left[\frac{1}{\omega - G_{\alpha\beta}/r^s}\rho^{(\text{int})}_\alpha\right]_r <\alpha|i'_1 j_2><j'_1 j_2|\beta> g_{j2} e^{-E_{j2}/kT}/Q_b, \tag{11}$$

where $G_{\alpha\beta} = G_\alpha - G_\beta$, i_2 and j_2 stand for all the quantum numbers of the bath molecule specifying its states, g_{j2} are the degeneracy factors due to nuclear spin, E_{j2} are the energies associated with the state $|j_2>$, and Q_b is the partition function for the bath molecules. The remaining summation over the external variables of the molecules is indicated by the trace with an index r. We note that the summation over the internal bath variables in the internal bath line space in Eq. (11) includes only the states $|i_2 i^\dagger_2>$ because of the assumption that the bath molecule is not involved in the transition.

2.2. The quasistatic approximation

We assume that the interaction between the absorber molecule and a bath molecule, $V(\vec{r})$, is

$$V(\vec{r}) = V_{\text{anis}}(\vec{r}) + V_{\text{is}}(r), \tag{12}$$

where $V_{\text{anis}}(\vec{r})$ is the leading term of the expansion of the anisotropic potential and $V_{\text{is}}(r)$ is a simple Lennard-Jones type model

$$V_{is}(r) = C\sigma^{-6}[(\sigma/r)^t + (\sigma/r)^6], \tag{13}$$

where C, σ and t are parameters which are consistent with values obtained from other data (Rosenkranz, 1985, 1987).

Based on the statistical theory in which the duration of a collision is assumed to be infinite and, therefore, which is valid in the far-wing limit, the relative motion of the two molecules is not treated quantum mechanically, rather one uses the quasistatic approximation. In this approximation, the trace with the index r in Eq. (11) is replaced by an integration over r, the separation between two interacting molecules, and the part of the density matrix related to the interaction, $\rho_\alpha^{(int)}$, is a statistical weight for a pair of molecules (the absorber and the bath molecule b) at the separation r and with their orientations specified by α; this is given by

$$\rho_\alpha^{(int)} = e^{-V_{\alpha\alpha}(r)/kT}/U, \tag{14}$$

where

$$\begin{aligned} V_{\alpha\alpha}(r) &= <\alpha|V_{anis}(\vec{r})|\alpha> + V_{is}(r) \\ &= G_\alpha/r^s + V_{is}(r). \end{aligned} \tag{15}$$

The normalization factor U is given by

$$\begin{aligned} U &= Tr[e^{-V_{\alpha\alpha}(r)/kT}]_{r\alpha} \\ &= \int_0^{r_{max}} e^{-V(\vec{r})/kT} d\vec{r}. \end{aligned} \tag{16}$$

In the last step in deriving Eq. (16), we have used the fact that the trace over rotational states related to the relative motion of the two molecules corresponds to a classical average over the angular variables of the relative motion. This expression can be rewritten in the form

$$\begin{aligned} U &= -\int_0^{r_{max}} (1 - e^{-V(\vec{r})/kT}) d\vec{r} + \int_0^{r_{max}} d\vec{r} \\ &= -\int_0^{r_{max}} (1 - e^{-V(\vec{r})/kT}) d\vec{r} + V, \end{aligned} \tag{17}$$

where V is the volume which can be replaced by $1/n_b$, i.e., by the inverse of the number density of bath molecules. Thus for moderate densities and temperatures, $U \cong 1/n_b$ and we obtain

$$\rho^{(int)} = n_b e^{-V(\vec{r})/kT}. \tag{18}$$

Therefore, within the quasistatic approximation, we have

$$Tr\left[\frac{1}{\omega-G_{\alpha\beta}/r^s}\rho_\alpha^{(\mathrm{int})}\right]_r=4\pi n_b\int_0^\infty r^2\mathrm{d}r\frac{1}{\omega-G_{\alpha\beta}/r^s}e^{-V_{\alpha\alpha}(r)/kT}. \tag{19}$$

With Eq. (19), the components of the resolvent operator $<(1)/(\omega-L_1)\rho^{(\mathrm{int})}>_b$ can be rewritten as

$$<i_1 j_1^\dagger|<\frac{1}{\omega-L_1}\rho^{(\mathrm{int})}>_b|i_1' j_1'^\dagger>=4\pi n_b\int_0^\infty r^2\mathrm{d}r\sum_{i_2 j_2}\sum_{\alpha\beta}<i_1 i_2|\alpha>$$

$$<\beta|j_1 i_2>\frac{1}{\omega-G_{\alpha\beta}/r^s}e^{-V_{\alpha\alpha}(r)/kT}\times<\alpha|i_1' j_2><j_1' j_2|\beta>g_{j2}e^{-E_{j2}/kT}/Q_b. \tag{20}$$

It is easy to obtain their imaginary parts with the well-known formal identity

$$\lim_{\epsilon\to 0}\frac{1}{\omega-\mathrm{L}_1+\mathrm{i}\epsilon}=\mathrm{P}\frac{1}{\omega-\mathrm{L}_1}-\mathrm{i}\pi\delta(\omega-\mathrm{L}_1), \tag{21}$$

where P indicates the Cauchy principal value of the integral and δ is a Dirac delta function having the Liouville operator $\omega-L_1$ as its argument; explicitly

$$Im<i_1 j_1^\dagger|<\frac{1}{\omega-L_1}\rho^{(\mathrm{int})}>_b|i_1' j_1'^\dagger> \tag{22}$$

$$=-4\pi^2 n_b\int_0^\infty r^2\mathrm{d}r\sum_{i_2 j_2}\sum_{\alpha\beta}<i_1 i_2|\alpha><\beta|j_1 i_2>\delta(\omega-G_{\alpha\beta}/r^s)e^{-V_{\alpha\alpha}(r)/kT}$$

$$\times<\alpha|i_1' j_2><j_1' j_2|\beta>g_{j2}e^{-E_{j2}/kT}/Q_b$$

$$=-4\pi^2 n_b\int_0^\infty r^2\mathrm{d}r\sum_{i_2 j_2}\sum_{\alpha\beta}<i_1 i_2|\alpha><\beta|j_1 i_2$$

$$>\frac{r^{s+1}}{s|G_{\alpha\beta}|}\delta[r-(G_{\alpha\beta}/\omega)^{1/s}]e^{-V_{\alpha\alpha}(r)/kT}$$

$$\times<\alpha|i_1' j_2><j_1' j_2|\beta>g_{j2}e^{-E_{j2}/kT}/Q_b$$

$$=-\frac{4\pi^2}{s}n_b\frac{1}{\omega}\sum_{i_2 j_2}\sum_{\alpha\beta}<i_1 i_2|\alpha><\beta|j_1 i_2$$

$$>(|G_{\alpha\beta}|/\omega)^{3/s}e^{-V_{\alpha\alpha}[(G_{\alpha\beta}/\omega)^{1/s}]/kT}$$

$$\times\Theta(G_{\alpha\beta}/\omega)<\alpha|i_1' j_2><j_1' j_2|\beta>g_{j2}e^{-E_{j2}/kT}/Q_b,$$

where $\Theta(x)$ is the unit step function.

2.3. The individual line shape functions

We introduce the individual line coupling functions, $\chi_{i_1j_1i'_1j'_1}(\omega)$, defined by

$$\chi_{i_1j_1i'_1j'_1}(\omega)\equiv\frac{4\pi^2}{s}n_b\sum_{i_2j_2}\sum_{\alpha\beta}\Theta(G_{\alpha\beta}/\omega)\omega^{(s-3)/s}|G_{\alpha\beta}|^{3/s}<i_1i_2|\alpha>$$

$$<\beta|j_1i_2>\times e^{-V_{\alpha\alpha}[(G_{\alpha\beta}/\omega)^{1/s}]/kT}<\alpha|i'_1j_2><j'_1j_2|\beta>g_{j_2}e^{-E_{j2}/kT}/Q_b. \quad (23)$$

Then the imaginary components of the resolvent operator $<(1)/(\omega'-L_1)\rho^{(\mathrm{int})}>_b$ can be simply expressed as

$$Im<i_1j_1^\dagger|<\frac{1}{\omega-L_1}\rho^{(\mathrm{int})}>_b|i'_1j'^\dagger_1>=-\frac{1}{\omega^2}\chi_{i_1j_1i'_1j'_1}(\omega). \quad (24)$$

With the Cauchy integral formula

$$f(a)=\frac{1}{2\pi i}\oint\frac{f(z)}{z-a}dz, \quad (25)$$

it is easy to carry out the integration in the spectral density and obtain

$$F(\omega)=\frac{1}{\pi}Im\frac{1}{2\pi i}\int_{-\infty}^{\infty}d\omega' Tr[\vec{\mu}_a\cdot\frac{1}{\omega-\omega'-L_a}\times<\frac{1}{\omega'-L_1}\rho^{(\mathrm{int})}>_b\rho^{(a)}\vec{\mu}_a]_a$$

$$=\frac{1}{\pi}\frac{1}{2\pi i}\int_{-\infty}^{\infty}d\omega'\sum_{i_1j_1}\sum_{i'_1j'_1}<j_1|\vec{\mu}_a|i_1>\frac{1}{\omega-\omega'-\omega_{i_1j_1}}Im<i_1j_1^\dagger|$$

$$<\frac{1}{\omega-L_1}\rho^{(\mathrm{int})}>_b|i'_1j'^\dagger_1>\times g_{i'_1}e^{-Ei'_1/kT}<i'_1|\vec{\mu}_a|j'_1$$

$$>/Q_a=\frac{1}{\pi}\frac{-1}{2\pi i}\int_{-\infty}^{\infty}d\omega'\sum_{i_1j_1}\sum_{i'_1j'_1}<j_1|\vec{\mu}_a|i_1>\frac{1}{\omega-\omega'-\omega_{i_1j_1}}\times\frac{1}{\omega'^2}\chi_{i_1j_1i'_1j'_1}(\omega')$$

$$\times g_{i'_1}e^{-Ei'_1/kT}<i'_1|\vec{\mu}_a|j'_1>/Q_a=\frac{1}{\pi}\sum_{i_1j_1}\sum_{i'_1j'_1}<j_1|\vec{\mu}_a|i_1>\frac{1}{(\omega-\omega_{i_1j_1})^2}\chi_{i_1j_1i'_1j'_1}$$

$$(\omega-\omega_{i_1j_1})g_{i_1}e^{-Ei'_1/kT}<i'_1|\vec{\mu}_a|j'_1>/Q_a. \quad (26)$$

We note that the arguments of each line coupling function in Eq. (26) take the desirable form after the Cauchy integration over ω' is carried out.

More conveniently, the spectral density can also be expressed in terms of the individual line shape functions as

$$F(\omega)=\frac{1}{\pi}\sum_{\omega_{ij}>0}\left\{\frac{1}{(\omega-\omega_{ij})^2}\chi_{ij}(\omega-\omega_{ij})\right.$$

$$\left.+e^{\hbar\omega_{ij}/kT}\frac{1}{(\omega+\omega_{ij})^2}\chi_{ji}(\omega+\omega_{ij})\right\}\rho_i|\mu_{ij}|^2. \quad (27)$$

Here the individual line shape functions are

$$\chi_{i_1j_1}(\omega)\equiv\frac{4\pi^2}{s}n_b\sum_m\sum_{m_{i_1}}\sum_{m_{j_1}}\sum_{\alpha\beta}\sum_{i_2}(<\alpha|i_1i_2><i_1|\mu_m|j_1>$$

$$<j_1i_2|\beta>)^*\Theta(G_{\alpha\beta/\omega})\omega^{(s-3)/s}|G_{\alpha\beta}| \quad (28)$$

$$\times e^{-V_{\alpha\alpha}[(G_{\alpha\beta}/\omega)^{1/s}]/kT}<\alpha|\rho^{(b)}\rho^{(a)}\mu_m|\beta>/\rho_{i_1}|\mu_{i_1j_1}|^2,$$

where m_{i_1} and m_{j_1} are the magnetic quantum numbers related to the state i and j, respectively; for simplicity we have omitted the subscript 1 which indicates the absorber molecule. If we define the symmetric individual line shape functions

$$\hat{\chi}_{i_1j_1}(\omega)\equiv e^{\hbar\omega/2kT}\chi_{i_1j_1}(\omega), \quad (29)$$

then the absorption coefficient $\alpha(\omega)$ can be written in the familiar form

$$\alpha(\omega)=n_a\sum_{\omega_{ij}>0}S_{ij}\frac{\omega sh(\hbar\omega/2kT)}{\omega_{ij}sh(\hbar\omega_{ij}/2kT)}\frac{1}{\pi}\left\{\frac{1}{(\omega-\omega_{ij})^2}\hat{\chi}_{ij}(\omega-\omega_{ij})\right.$$

$$\left.+\frac{1}{(\omega+\omega_{ij})^2}\hat{\chi}_{ji}(\omega+\omega_{ij})\right\}, \quad (30)$$

where S_{ij} are the line strengths.

We note that the individual line shape functions are not even functions of their argument

$$\hat{\chi}_{ij}(\omega)=\hat{\chi}_{ji}(-\omega) \text{ but } \hat{\chi}_{ij}(\omega)\neq\hat{\chi}_{ij}(-\omega). \quad (31)$$

implying that the line shapes are asymmetric about their centers.

2.4. The band independence approximation

In the present paper, we are interested in the case in which the absorber molecule has a large permanent dipole moment and the leading term in the anisotropic interaction is due to the interaction between this dipole and the leading multipole moment of the bath molecule. In light of the fact that the matrix elements of the dipole moment of the absorber molecule between different vibrational states are at least an order of magnitude smaller that those between the same vibrational states, and that the matrix elements of the dipole moment between the same vibrational states are only slightly dependent on its vibrational quantum number, we can assume that the matrix of G takes a block diagonal form. Using this assumption, the lines belonging to the different vibrational bands are not coupled

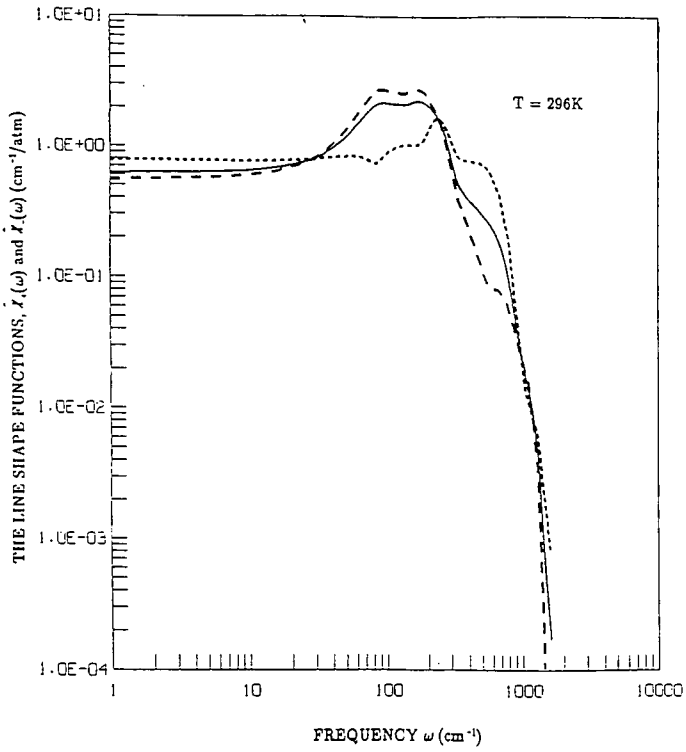

Fig. 1. The positive and negative frequency resonance average line shape functions for H_2O–H_2O self-broadening (in units of cm^{-1}/atm): $\hat{\chi}_+(\omega)$ (dashed curve) and $\hat{\chi}_-(\omega)$ (dotted curve), as a function of frequency ω (in units of cm^{-1}) calculated for $T=296$ K. The solid curve is the intensity-weighted average line shape function.

to each other, and the lines within each band are coupled in the same way. More precisely, the latter means that the individual line shape functions are common for all the rotational lines in a given band. If we denote those obtained from the pure rotational band by $\chi_{ij}(\omega)$ where the indices i and j indicate the rotational quantum numbers only and indicate the vibrational quantum numbers by v_i and v_j, then the general expression of the individual line shape functions can be written as

$$\chi_{V_iiV_jj}(\omega)=\chi_{V_i,iV_j,j}(\omega)=X_{ij}(\omega) \tag{32}$$

Based on the argument above, the total spectral density can be expressed as the sum of its components corresponding to each individual band

$$F(\omega)=\sum_{V_iV_j} F_{V_iV_j}(\omega). \tag{33}$$

Furthermore, the components of the spectral density, $F_{V_iV_j}(\omega)$, can be expressed as

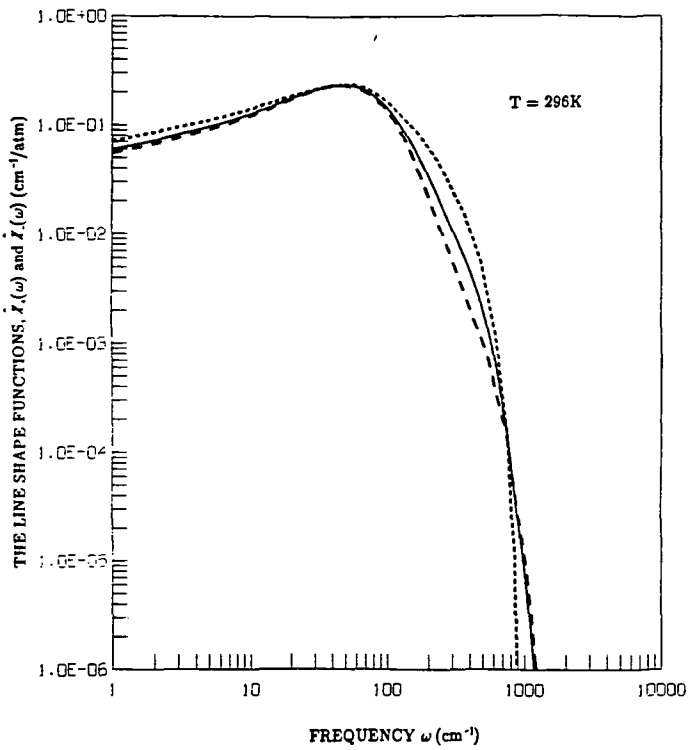

Fig. 2. The positive and negative frequency resonance average line shape functions for H_2O–N_2 foreign-broadening (in units of cm^{-1}/atm): $\hat{\chi}_+(\omega)$ (dashed curve) and $\hat{\chi}_-(\omega)$ (dotted curve), as a function of frequency ω (in units of cm^{-1}) calculated for $T=296$ K. The solid curve is the intensity-weighted average line shape function.

$$F_{V_iV_j}(\omega)=\frac{1}{\pi}\sum_{\omega_{V_{ii},V_{jj}}>0}\left\{\frac{1}{(\omega-\omega_{V_{ii},V_{jj}})^2}\chi_{ij}(\omega-\omega_{V_{ii},V_{jj}})\right.$$
$$\left.+e^{\hbar\omega_{V_{ii},V_{jj}}/kT}\frac{1}{(\omega+\omega_{V_{ii},V_{jj}})^2}\chi_{ji}(\omega+\omega_{V_{ii},V_{jj}})\right\}\rho_{V_{ii}}|\mu_{V_{ii},V_{jj}}|^2. \quad (34)$$

Finally, the total absorption coefficient can also be expressed as the superposition of the components corresponding to each individual band; i.e.

$$\alpha(\omega)=\sum_{V_iV_j}\alpha_{V_iV_j}(\omega), \quad (35)$$

where

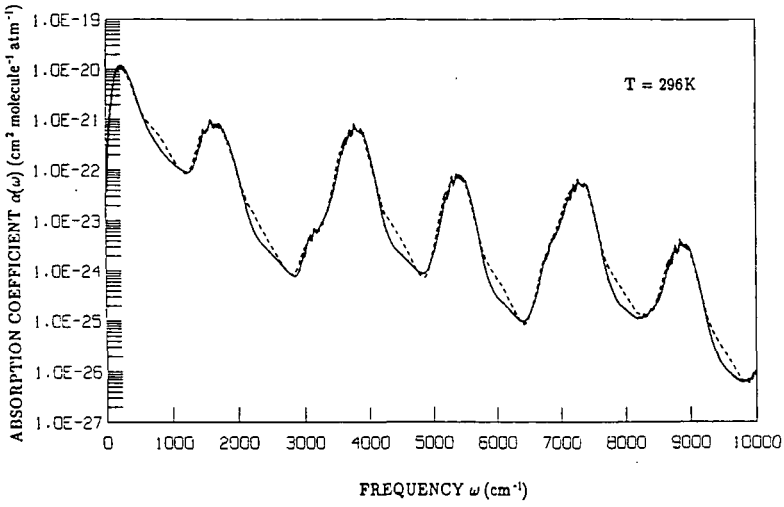

Fig. 3. The H_2O–H_2O absorption coefficient $\alpha(\omega)$ (in units of cm^2 $molecule^{-1}$ atm^{-1}) as a function of frequency ω (in units of cm^{-1}) calculated for $T = 296$ K. The results obtained from the two averaged line shape functions are the solid curve, and the results from the intensity-weighted average line shape function are the dotted curve.

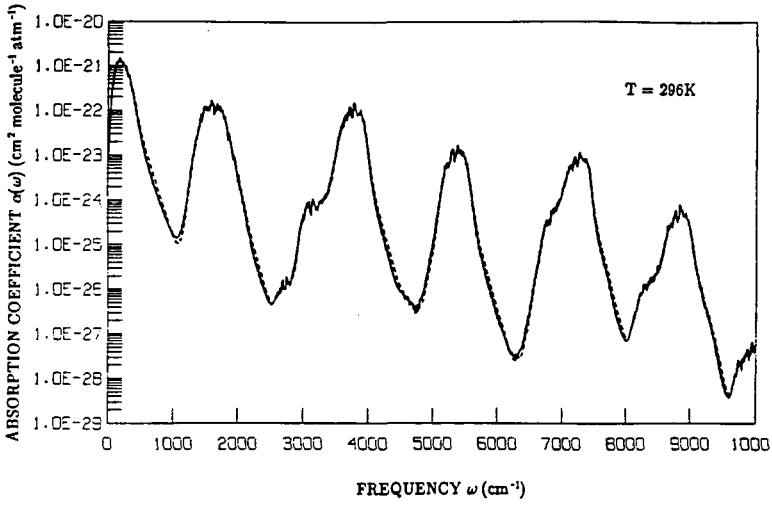

Fig. 4. The H_2O–N_2 absorption coefficient $\alpha(\omega)$ (in units of cm^2 $molecule^{-1}$ atm^{-1}) as a function of frequency ω (in units of cm^{-1}) calculated for $T = 296$ K. The results obtained from the two averaged line shape functions are the solid curve, and the results from the intensity-weighted average line shape function are the dotted curve.

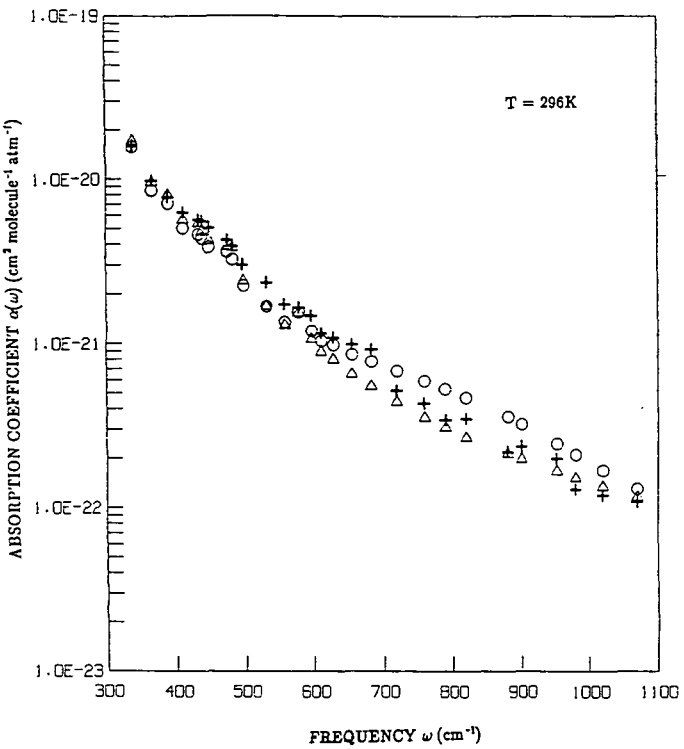

Fig. 5. The H_2O–H_2O absorption coefficient $\alpha(\omega)$ (in units of cm^2 $molecule^{-1}$ atm^{-1}) as a function of frequency ω (in units of cm^{-1}) calculated for $T=296$ K; the experimental values of Burch et al. (1984, 1985) are denoted by +, while Δ corresponds to the theoretical values calculated with two line shape functions, and O to those calculated with one line shape function.

$$\alpha_{V_iV_j}(\omega)=n_a\sum_{\omega_{V_{ii},V_{jj}}>0}S_{V_{ii},V_{jj}}\frac{\omega sh(\hbar\omega/2kT)}{\omega_{V_{ii},V_j}sh(\hbar\omega_{V_{ii},V_{jj}}/2kT)}\frac{1}{\pi}\left\{\frac{1}{(\omega-\omega_{V_{ii},V_{jj}})^2}\right.$$

$$\left.\hat{\chi}_{ij}(\omega-\omega_{V_{ii},V_{jj}})+\frac{1}{(\omega+\omega_{V_{ii},V_{jj}})^2}\hat{\chi}_{ji}(\omega+\omega_{V_{ii},V_{jj}})\right\}. \tag{36}$$

In general, the line shape functions decrease very rapidly when their arguments increase; therefore, at the frequencies of interest the main contributions to the total absorption coefficient come from the nearby strong bands only. This is especially true for the cases in which the leading anisotropic interaction between two interacting molecules is weak.

In practical calculations, we can also introduce the positive and negative frequency resonance-average line shape functions (Ma and Tipping, 1991, 1992a, b), $\hat{\chi}_+(\omega)$ and $\hat{\chi}_-(\omega)$, which are common for every band and which simplify the calculation of the absorption coefficient. We note that the first terms in the

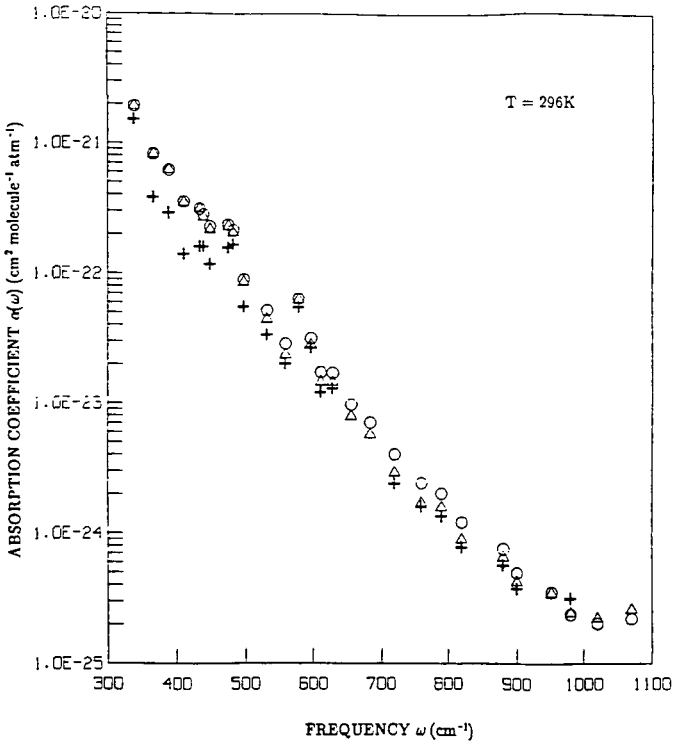

Fig. 6. The H_2O–N_2 absorption coefficient $\alpha(\omega)$ (in units of cm^2 $molecule^{-1}$ atm^{-1}) as a function of frequency ω (in units of cm^{-1}) calculated for $T=296$ K; the experimental values of Burch et al. (1984, 1985) are denoted by +, while Δ corresponds to the theoretical values calculated with two line shape functions, and O to those calculated with one line shape function.

curly bracket in Eq. (36) are related to the positive frequency resonances and the second terms to the negative frequency resonance. We define the intensity-weighted positive frequency resonance-average line shape function by

$$\hat{\chi}_+(\omega) \equiv \sum_{\omega_{ij}>0} \hat{\chi}_{ij}(\omega)\rho_i |\mu_{ij}|^2 / \sum_{\substack{ij \\ E_i > E_j}} \rho_i |\langle i|\mu_m|j\rangle|^2 \tag{37}$$

$$= \frac{4\pi^2}{s} n_b \sum_{\substack{i_1 j_1 \\ E_{i_1} > E_{j_1}}} \sum_m \sum_{\alpha\beta} \sum_{i_2} (\langle \alpha|i_1 i_2\rangle \langle i_1|\mu_m|j_1\rangle$$

$$\langle j_1 i_2|\beta\rangle)^* \Theta(G_{\alpha\beta}/\omega)\omega^{(s-3)/s}|G_{\alpha\beta}|$$

$$\times e^{-\hbar\omega[(G_\alpha+G_\beta)/(G_\alpha-G_\beta)]/2kT - V_{is}[(G_{\alpha\beta}/\omega)^{1/3}]/kT}$$

$$\times \langle \alpha|\rho^{(b)}\rho^{(a)}\mu_m|\beta\rangle / \sum_{\substack{ij \\ E_i > E_j}} \rho_i |\langle i|\mu_m|j\rangle|^2.$$

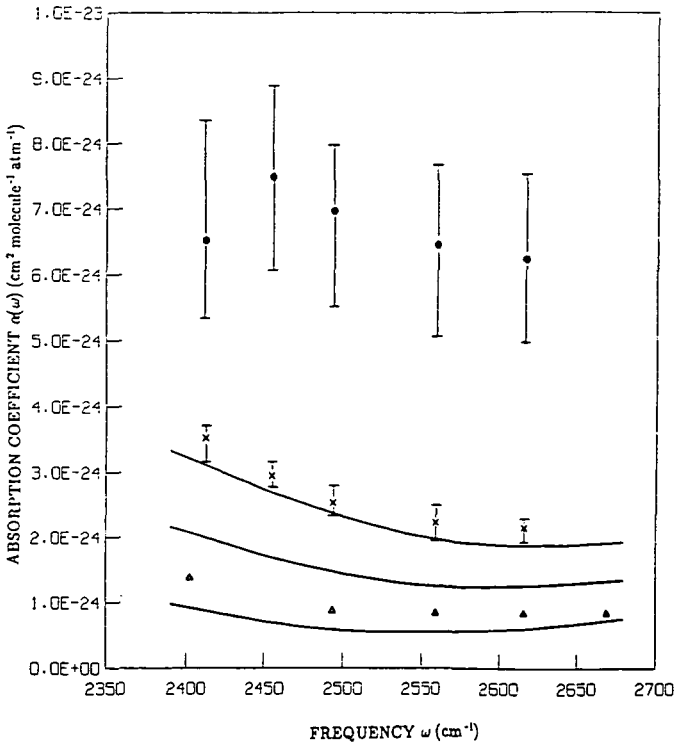

Fig. 7. Comparison between the H_2O–H_2O theoretical values and the laboratory experimental data of Burch et al. (1984, 1985) for three temperatures in the spectral range 2400 $cm^{-1} < \omega < 2700$ cm^{-1}. The solid curves are the theoretical results for temperatures $T = 296$ K, 328 K and 428 K, from the top to the bottom, respectively. The corresponding experimental data are denoted by 1, x, and Δ, respectively.

Similarly, we define the intensity-weighted negative frequency resonance-average line shape function by

$$\hat{\chi}_-(\omega) \equiv \sum_{\omega_{ij}>0} \hat{\chi}_{ji}(\omega)\rho_j |\mu_{ji}|^2 / \sum_{\substack{ij \\ E_i > E_j}} \rho_j |\langle j|\mu_m|i\rangle|^2 \tag{38}$$

$$= \frac{4\pi^2}{s} n_b \sum_{\substack{i_1 j_1 \\ E_{i_1} < E_{j_1}}} \sum_m \sum_{\alpha\beta} \sum_{i_2} (\langle \alpha | i_1 i_2 \rangle \langle i_1 | \mu_m | j_1 \rangle$$

$$\langle j_1 i_2 | \beta \rangle)^* \Theta(G_{\alpha\beta}/\omega)\omega^{(s-3)/s} |G_{\alpha\beta}|$$

$$\times e^{-\hbar\omega[(G_\alpha + G_\beta)/(G_\alpha - G_\beta)]/2kT - V_{is}[(G_{\alpha\beta}/\omega)^{1/3}]/kT}$$

$$\times \langle \alpha | \rho^{(b)} \rho^{(a)} \mu_m | \beta \rangle / \sum_{\substack{ij \\ E_i < E_j}} \rho_i |\langle i|\mu_m|j\rangle|^2.$$

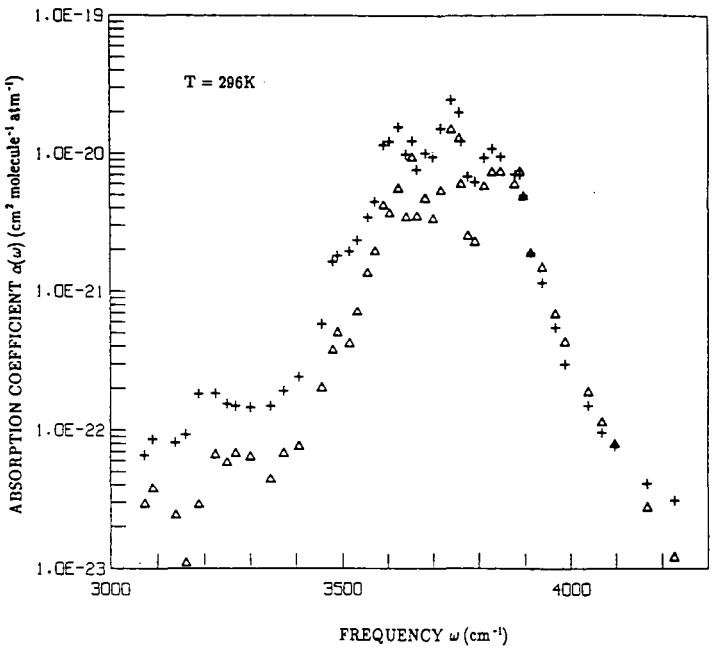

Fig. 8. Comparison between the H_2O–H_2O theoretical values and the laboratory experimental data of Burch et al. (1984, 1985) for $T=296$ K in the spectral range $3000\ \text{cm}^{-1}<\omega<4300\ \text{cm}^{-1}$. The theoretical values are denoted by Δ and the experimental values by +, respectively.

We need only to evaluate $\hat{\chi}_+(\omega)$ and $\hat{\chi}_-(\omega)$ for $\omega>0$ since the values of these functions for $\omega<0$ are approximate equal or equal to their partner's value for $\omega>0$; i.e., $\hat{\chi}_+(-\omega)\cong\hat{\chi}_-(\omega)$. If we do not distinguish between these two averages, we define the intensity-weighted line shape function $\chi(\omega)$

$$\hat{\chi}(\omega)\equiv\sum_{ij}\hat{\chi}_{ij}(\omega)\rho_i|\mu_{ij}|^2/\sum_{ij}\rho_i|<i|\mu_m|j>|^2=\frac{4\pi^2}{s}n_b\sum_{\alpha\beta}<\alpha|\mu_m|\beta>^*\Theta(G_{\alpha\beta}/\omega)\omega^{(s-3)/s}|G_{\alpha\beta}|^{3/8}\times e^{-\hbar\omega[(G_\alpha+G_\beta)/(G_\alpha-G_\beta)]/2kT-V_{is}[(G_{\alpha\beta}/\omega)^{1/3}]/kT}\times<\alpha|\rho^{(b)}\rho^{(a)}\mu_m|\beta>/\sum_{ij}\rho_i|<i|\mu_m|j>|^2. \tag{39}$$

With the two average line shape functions, the components of the absorption coefficient can be written

$$\alpha_{V_iV_j}(\omega)=n_a\sum_{\omega_{Vii,Vjj}>0}S_{V_{ii},V_{jj}}\frac{\omega sh(\hbar\omega/2kT)}{\omega_{V_{ii},V_{jj}}sh(h\omega_{vii,vjj}/2kT)}\frac{1}{\pi}\left\{\frac{1}{(\omega-\omega_{V_{ii},V_{jj}})^2}\hat{\chi}_+(\omega-\omega_{V_{ii},V_{jj}})+\frac{1}{(\omega+\omega_{V_{ii},V_{jj}})^2}\hat{\chi}_-(\omega+\omega_{V_{ii},V_{jj}})\right\}. \tag{40}$$

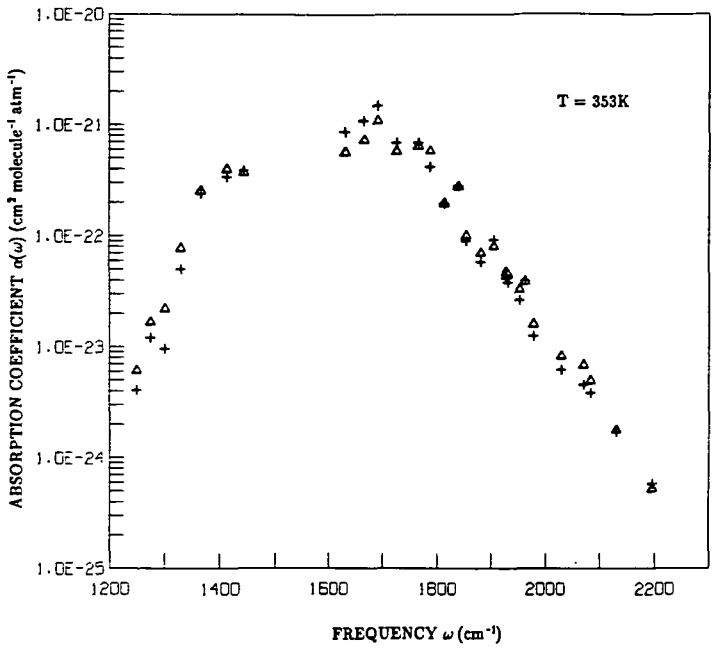

Fig. 9. Comparison between the H_2O–N_2 theoretical values and the laboratory experimental data of Burch et al. (1984, 1985) for $T=353$ K in the spectral range $1200\ cm^{-1}<\omega<2300\ cm^{-1}$. The theoretical values are denoted by Δ and the experimental values by +, respectively.

Because these two averaged line shape functions are common for all the bands, and they fall off very rapidly as their arguments increase, the continuum absorption is mainly determined by the nearest and strongest two bands; that is the one on the low-frequency and the one on the high-frequency side of each window. We expect that the basic features of the absorption in all the windows, including the temperature dependence, should be, more or less, similar to each other. However, their magnitudes, which are roughly proportional to the total intensities of the nearest bands, are expected to be different, generally decreasing as the frequency ω increases.

3. Computational results of the water continuum absorption

Using the theory outlined above together with the accurate position and intensity data of the H_2O transitions (Rothman et al., 1987), and the dipole moment of H_2O, $\mu=1.8546\ D$, the quadrupole moment $Q=-1.04\ ea_o^2$ of N_2, and the same parameters of the isotropic interaction used by Rosenkranz (1985, 1987) ($C/k=8.0\times10^5$ Å^6 K, $s=48$, and $\sigma=3.13$ Å for H_2O–H_2O; and $C/k=8.2\times10^5$ Å^6 K, $s=9$, and $\sigma=2.94$ Å for H_2O–N_2), we have calculated the positive and negative frequency resonance average line shape functions for H_2O–H_2O and for H_2O–N_2

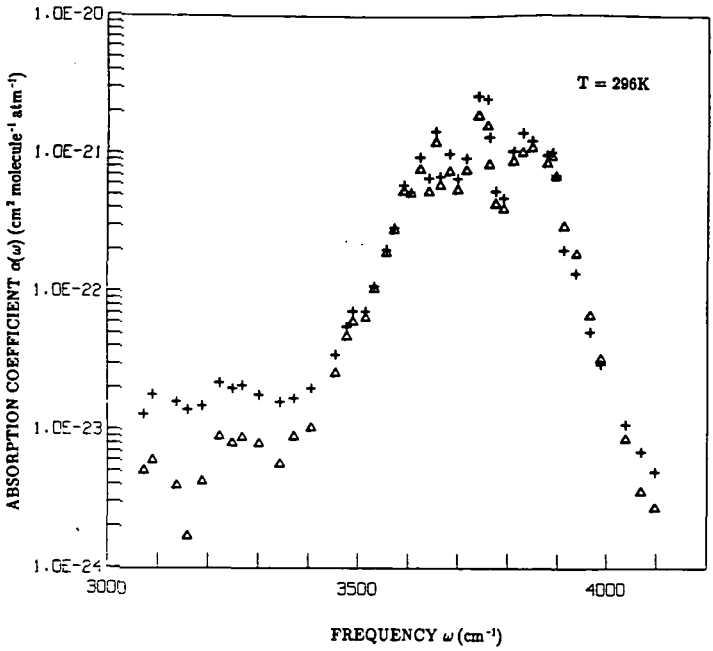

Fig. 10. Comparison between the H_2O–N_2 theoretical values and the laboratory experimental data of Burch et al. (1984, 1985) for $T=296$ K in the spectral range $3000\ cm^{-1} < \omega < 4100\ cm^{-1}$. The theoretical values are denoted by Δ and the experimental values by +, respectively.

as shown in Figs. 1 and 2 for $T=296$K. Also shown are the corresponding results obtained from the theory of Rosenkranz (1985, 1987). These functions have the same general shape as the empirical χ functions deduced from laboratory and atmospheric data (Clough et al., 1989) and used in many atmospheric codes. However, one cannot compare these functions directly because of different mathematical expressions for the absorption coefficient [the use of the hyperbolic tanh instead of sinh, cf. Eq. (40)], and the different treatment of the contributions from local lines (i.e., those within some cutoff frequency, typically $\pm 25\ cm^{-1}$).

The corresponding theoretical absorption coefficients, $\alpha(\omega)$, for frequencies to 10 000 cm^{-1} are shown in Figs. 3 and 4, respectively, for self- and N_2-broadening at $T=296$ K. We note that these results vary over 5 orders of magnitude in this limited frequency range. Similar results have been obtained for other temperatures in the range $200\ K < T < 700\ K$ but are not shown. In order to assess the importance of the far-wing contribution to atmospheric measurements, we first compare our results to the most comprehensive set of laboratory data, i.e., those of Burch and co-workers (1971, 1974, 1975, 1982, 1984, 1985).

4. Comparison between theory and experiment, preliminary atmospheric validations and conclusions

The theoretical absorption coefficients for self- and N_2-broadening are compared with the experimental results of Burch and co-workers in Figs. 5–10. From

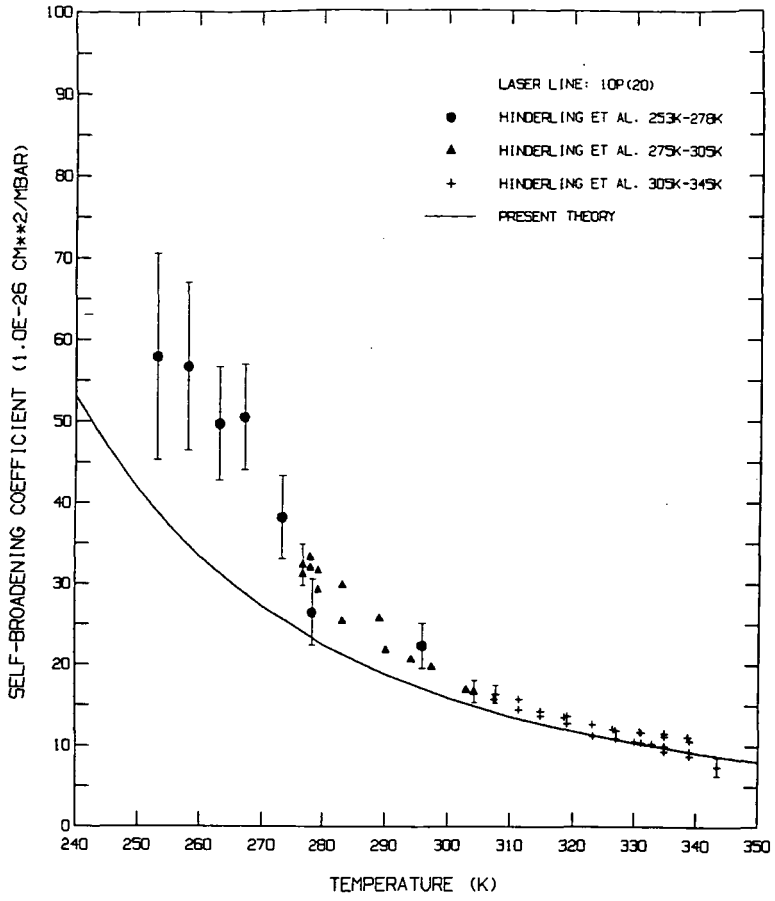

Fig. 11. Comparison between the theoretical temperature dependence and the laboratory data of Hinderling et al. (1987) at the 10P(20) CO_2 laser line frequency of 944.195 cm^{-1}.

these and other comparisons (Ma and Tipping, 1991, 1992a, b), we can draw the following conclusions: (i) Using the different positive and negative resonance average line shape functions gives better results than using a single average line shape function; (ii) The temperature dependence for this limited range of T is well described by the theory (in fact, the agreement is generally better for higher temperatures where the measured absorption is greater due to the increased vapor pressure and where the corresponding experimental uncertainties are lower); (iii) The agreement in the $300 < \omega < 1100$ cm^{-1} region is very good for both self- and N_2-broadening; (iv) The agreement in the $2400 < \omega < 2700$ cm^{-1} region is not as good, but the absolute magnitude of the continua are smaller than those in the $300 < \omega < 1100$ cm^{-1} region by approximately a factor of 100 (see Figs. 3 and 4), and the corresponding experimental uncertainties are much larger; (v) The agreement for measurements made near the centers of vibration-rotational bands

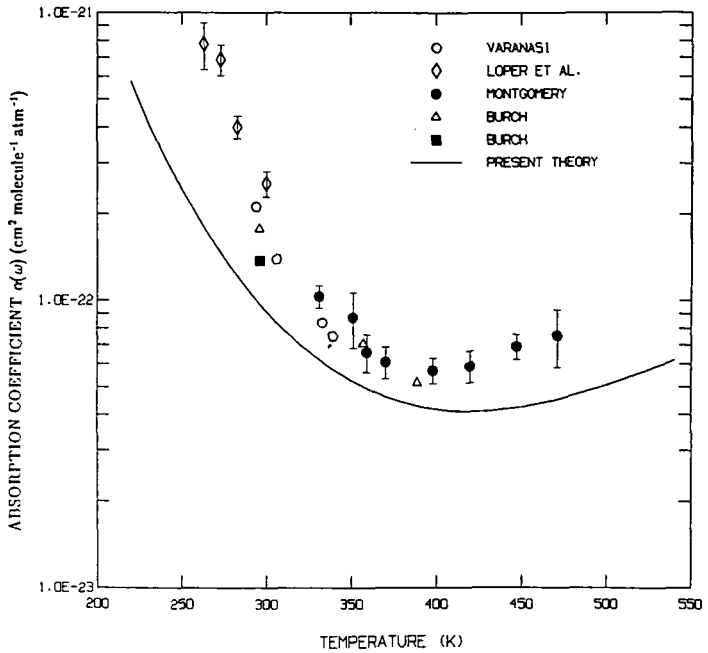

Fig. 12. Comparison between the theoretical temperature dependence and various laboratory data: ◇ Loper et al. (1983); ● Momtgomery (1978); △ Burch et al. (1971); ■ Burch data, cited by Roberts et al. (1976), all for $\omega \cong 1203\ cm^{-1}$; ○ Varanasi (1988b) for $\omega \cong 1000\ cm^{-1}$.

(1200–2200 cm^{-1} and 3000–4200 cm^{-1}) show greater scatter than measurements made between the bands; (vi) Most of the theoretical values are below the corresponding experimental measurements. We will return to this last point later.

In order to investigate the temperature dependence in more detail over a wider range of T, we compare in Fig. 11 the theoretical calculations with the experimental results of Hinderling et al. (1987), obtained using the 10P(20) laser line of CO_2 having a frequency of 944.195 cm^{-1}. The results are similar to those obtained using the data of Burch and co-workers; viz., the theoretical values are systematically lower than the experimental values, and the agreement is generally better at higher temperatures where the experimental uncertainties are smaller. Similar results obtain for comparisons made with other laser lines. In Fig. 12, we show a comparison for the temperature dependence of the self absorption coefficient at frequencies near 1203 cm^{-1} with experimental data obtained by a number of researchers using different experimental techniques (Burch et al., 1971; Montgomery, 1978; Loper et al., 1983). Also shown are some data from Varanasi (1988b) for a frequency near 1000 cm^{-1}. It is clear that the theoretical results reproduce the general trend very well, but underestimate the magnitude by 30% or so. We note that in contrast to the empirical model of Roberts et al. (1976) or predictions made assuming the dimer model, the absorption coefficient shows a positive slope for temperatures above 400 K that is corroborated by the present

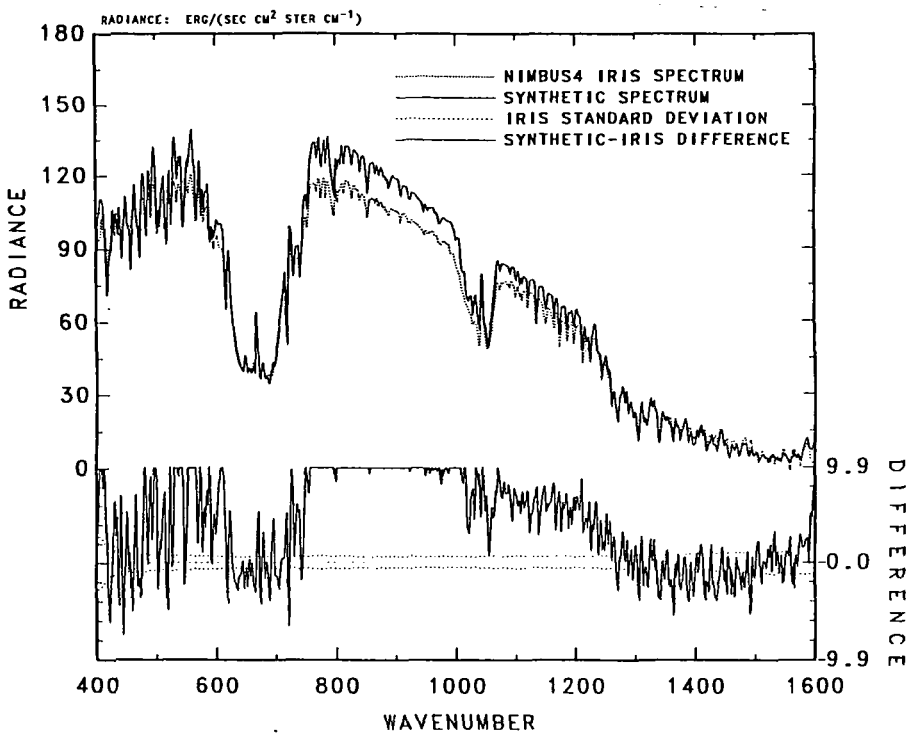

Fig. 13. Comparison between the Nimbus-4 IRIS satellite radiance spectrum in the 400 $cm^{-1} < \omega < 1600$ cm^{-1} spectral region and the line-by-line synthetic spectrum calculated without the inclusion of the far-wing water absorption; the difference is plotted in the lower part of the figure together with the IRIS standard deviation.

theoretical calculations. This change of slope with temperature depends sensitively on the frequency considered.

Bolstered by the good agreement between theory and laboratory data, we now discuss some preliminary validations of the theoretically calculated continua using atmospheric measurements. In Fig. 13 we show the radiance of the Earth as measured by the Nimbus-4 IRIS spectrometer in the $400 < \omega < 1600$ cm^{-1} region. Also shown is the predicted synthetic spectrum obtained using a line-by-line calculation without including the effects of the water continuum (Carlson and Lacis, 1992). For clarity, the difference between these is plotted in the lower part of the figure along with the IRIS standard deviation. As apparent from the figure, large differences are observed. In Fig. 14, we show a similar comparison except that the synthetic spectrum was calculated including the theoretical H_2O–H_2O continuum. The differences are dramatically reduced, especially in the important 700–1200 cm^{-1} region. Many of the remaining sharp differences arise from line mixing (e.g. in CO_2 Q branches) or from other trace molecular species not included in the synthesis. We note that similar comparisons using other continua, for instance that of Roberts et al. (1976) or the CKD model (Clough et al., 1989)

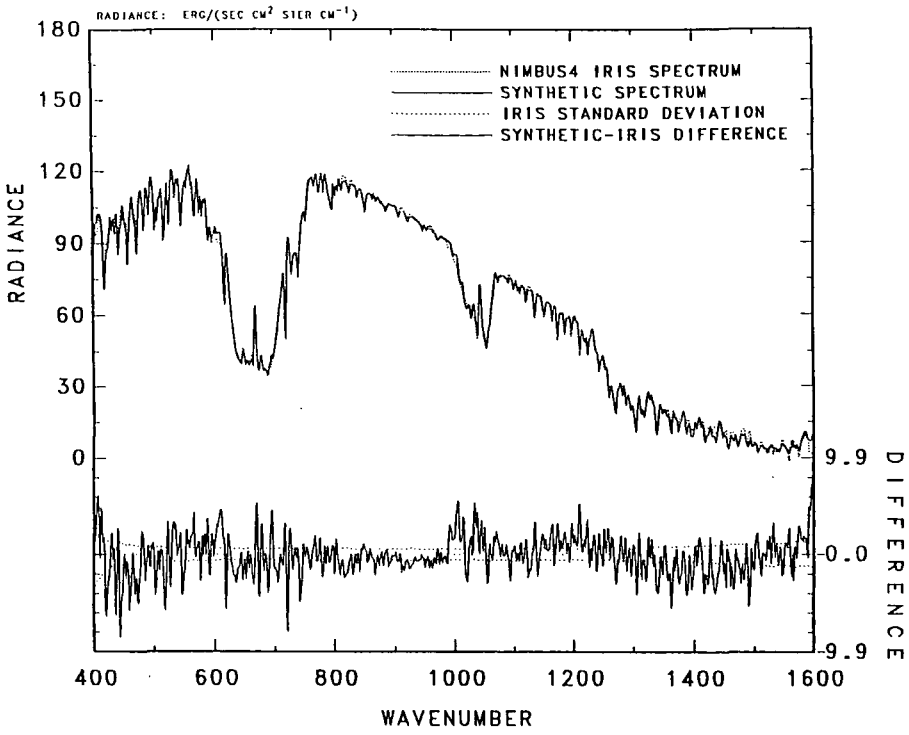

Fig. 14. The same as Fig. 13 except that the synthetic spectrum was calculated by including the far-wing water absorption.

would show similar reductions in the difference spectrum. This is obvious since the above mentioned continua are based primarily on the data of Burch et al. and the present theoretical values are in substantial agreement with this data in the spectral region covered by the IRIS instrument. Such agreement is not assured in other spectral regions, or more particularly, for other temperatures (Hartmann et al., 1993).

As a result of the comparisons discussed above and others not shown, we can draw several general conclusions concerning the contributions of far-wing absorption to the observed water continuum. The first and most important conclusion is that within the framework of the present theory and without the introduction of arbitrary adjustable parameters, we obtain generally good agreement with both laboratory and atmospheric data over a wide range of frequencies and temperatures. Thus we feel that this mechanism is the major source of the observed continuum absorption. As noted above, while the agreement between theory and measurements made near the band centers is generally good, there appears to be a systematic underestimate of the absorption. There are two possible theoretical interpretations for this discrepancy: the near wings of the strong vibration-rotational lines calculated using the quasistatic approximation may differ signifi-

cantly from the true line shapes, or there may be another mechanism producing absorption near the line centers. Both of these effects are currently under investigation. Corrections to the near-wing line shape resulting from the non-commutative term neglected in Eq. (3) and from the effects of molecular motion neglected in the quasistatic approximation would increase the near-wing absorption while leaving the far wings unchanged. We are also investigating the role and magnitude of interference effects associated with the allowed and the collision-induced dipoles. Such effects are known to play an important role in the spectra of HD (Herman et al., 1979).

In conclusion, we note that much progress on the theoretical understanding of the water continuum has been made. The far-wing absorption is the primary mechanism responsible for the water continuum and this is described reasonably well within the framework of the present theory. However, improvements to the theory and the possible inclusion of other mechanisms to calculate the absorption due to the near wings of spectral lines are needed. Finally, we would like to stress the need for more accurate experimental data (laboratory and atmospheric). When such data are available, and after the refinements discussed above are made, one can vary the input parameters for the isotropic interaction (the Lennard-Jones parameters) or even implement a different isotropic interaction and see if the discrepancies between theory and experiment can be reduced. No such optimization has been done in the present work because the differences between theory and experiment are well within the combined limits of errors, given the difficulties of the measurements and the mathematical approximations made in calculating the theoretical results.

Acknowledgments

This work was supported in part by the Department of Energy Interagency Agreement under the Atmospheric Radiation Measurement Program. One author (R.H.T.) wishes to thank Dr. Daniel Bershader, Director of the NASA-Ames ASEE Summer Faculty Program, for the award of a fellowship during which this work was carried out. We would also like to thank Drs. Barbara Carlson and Andy Lacis, NASA Goddard Space Flight Center, for providing the Nimbus-4 IRIS comparisons.

References

Birnbaum, G., 1985. Phenomena Induced by Intermolecular Interactions. Plenum, New York, N.Y.

Burch, D.E., Gryvnak, D.A. and Pembrook, J.D., 1971. Investigation of the Absorption of Atmospheric Gases. AFCRL-TR-71-0124.

Burch, D.E., Gryvnak, D.A. and Gates. F.J., 1974. Continuous Absorption by H_2O between 330 and 825 cm^{-1}. AFCRL-TR-74-0337.

Burch, D.E., Gryvnak, D.A. and Pembrook, J.D., 1975. Infrared Absorption by H_2O, NO_2 and N_2O_4. AFCRL-TR-75-0420.

Burch, D.E., 1982. Continuum Absorption by H_2O. AFGL-TR-81-0300.

Burch, D.E. and Alt, R.L., 1984. Continuous Absorption by Water in the 700–1200 cm^{-1} and 2400–2800 cm^{-1} windows. AFGL-TR-84-0128.

Burch, D.E., 1985. Absorption by H_2O in Narrow Windows between 3000 and 4200 cm^{-1}. AFGL-TR-85-0036.

Carlon, H., 1981. Infrared absorption by molecular clusters in water vapor. J. Appl. Phys., 52: 3111–3115.

Carlson, B.E. and Lacis, A.A., 1992. Private communication.

Clough, S.A., Kneizys, F.X., Davies, R., Gamache, R. and Tipping, R., 1980. Theoretical line shape for H_2O vapor in the infrared and millimeter regions. In: A. Deepak, T.D. Wilkerson and L.H., Ruhnke (Editors), Atmospheric Water Vapor. Academic Press, New York, pp. 25–46.

Clough, S.A., Davies, R.W. and Tipping, R.H., 1983. The line shape for collisionally broadened molecular transitions: A quantum theory satisfying the fluctuation dissipation theorem. In: Proc. 6th Conf. Spectral Line Shapes. Gruyter, New York, pp. 553–568.

Clough, S.A., Kneizys, F.X. and Davies, R.W., 1989. Line shape and the water continuum. Atmos. Res., 23: 229–241.

Davies, R.W., Tipping, R.H. and Clough, S.A., 1982. The dipole autocorrelation function for molecular pressure broadening: A quantum theory which satisfies the fluctuation-dissipation theorem. Phys. Rev., A 26: 3378–3394.

Deepak, A., Wilkerson, T.D. and Ruhnke, L.H. (Editors), 1980. Atmospheric Water Vapor. Academic Press, New York.

Elsasser, W.M., 1938. Far infrared absorption of atmospheric water vapor. *Astrophys. J.* 87: 497–507.

Fano, U., 1963. Pressure broadening as a prototype of relaxation. Phys. Rev., 131: 259–268.

Grant, W.B., 1990. Water vapor absorption coefficient in the 8–13 μm spectral region: A critical review. Appl. Opt., 29: 451–462.

Hartmann, J.M., Perrin, M.Y., Ma, Q. and Tipping, R.H., 1993. The infrared continuum of pure water vapor: Calculations and high-temperature measurements. J. Quant. Spectrosc. Rad. Trans., 49: 675–691.

Herman, R.M, Tipping, R.H. and Poll, J.D., 1979. Shape of the R and P lines in the fundamental band of gaseous HD. Phys. Rev., A 20: 2006–2012.

Hinderling, J., Sigrist, M.W. and Kneubuhl, F.K., 1987. Laser-photoacoustic spectroscopy of water-vapor continuum and line absorption in the 8 to 14 μm atmospheric window. Infrared Phys., 27: 63–120.

Kilsby, C.G., Edwards, D.P., Saunders, R.W. and Foot, J.S., 1992. Water–vapour continuum absorption in the tropics: Aircraft measurements and model comparisons. Q. J. R. Meteorol. Soc., 118: 715–748.

Liebe, H.J., 1989. MPM-an atmospheric millimeter-wave propagation model. Int. J. IR and MM Waves, 10: 631–650.

Loper, G.L., O'Neill, M.A. and Gelbawachs, J.A., 1983. Water–vapor continuum CO_2 laser absorption spectra between 27°C and −10°C. Appl. Opt., 23: 3701–3710.

Ma, Q. and Tipping, R.H., 1990a. The atmospheric water continuum in the infrared: Extension of the statistical theory of Rosenkranz. J. Chem. Phys., 93: 7066–7075.

Ma, Q. and Tipping, R.H., 1990b. Water vapor continuum in the millimeter spectral region. J. Chem. Phys., 93: 6127–6139.

Ma, Q. and Tipping, R.H., 1991. A far wing line shape theory and its application to the water continuum absorption in the infrared region. I. J. Chem. Phys., 95: 6290–6301.

Ma, Q. and Tipping, R.H., 1992a. A far wing line shape theory and its application to the water vibrational bands. II. J. Chem. Phys., 96: 8655–8663.

Ma, Q. and Tipping, R.H., 1992b. A far wing line shape theory and its application to the foreign-broadened water continuum absorption. III. J. Chem. Phys., 97: 818–828.

Ma, Q. and Tipping, R.H., 1994. The detailed Balance Requirement and General Empirical Formalisms for Continuous Absorption. J. Quant. Spectrosc. Rad. Trans. 34:.

Montgomery, G.P., 1978. Temperature dependence of infrared absorption by the water vapor continuum near 1200 cm^{-1}. Appl. Opt., 17: 2299–2303.

Nordstrom, R.J. and Thomas, M.E., 1980. The water continuum as wings of strong absorption lines. In: A. Deepak, T.D. Wilkerson and L.H. Ruhnke (Editors), Atmospheric Water Vapor. Academic Press, New York, pp. 77–100.

Penner, S. and Varanasi, P., 1967. Spectral absorption coefficients in the pure rotational spectrum of water vapor. J. Quant. Spectrosc. Radiat. Trans., 7: 687–690.

Roberts, R.E., Selby, J.E.A. and Biberman, L.M., 1976. Infrared continuum absorption by atmospheric water vapor in the 8–12 μm window. Appl. Opt., 15: 2085–2090.

Rosenkranz, P.W., 1985. Pressure broadening of rotational bands. I. A statistical theory. J. Chem. Phys., 83: 6139–6144.

Rosenkranz, P.W., 1987. Pressure broadening of rotational bands. II. Water vapor from 300 to 1100 cm^{-1}. J. Chem. Phys., 87: 163–170.

Rothman, L.S., Gamache, R.R., Goldman, A., Brown, L.R., Toth, R.A., Pickett, H.M., Poynter, R.L., Flaud, J.-M., Camy-Peyret, C., Barbe, A., Husson, N., Rinsland, C.P. and Smith, M.A.H., 1987. The HITRAN database: 1986 edition. Appl. Opt., 26: 4058–4097.

Thomas, M.E., 1990. Infrared- and millimeter-wavelength continuum absorption in the atmospheric windows: Measurements and models. Infrared Phys., 30: 161–174.

Thomas, M.E. and Nordstrom, R.J., 1982a. The N_2-broadened water vapor absorption line shape and infrared continuum absorption — I. Theoretical development. J. Quant. Spectrosc. Rad. Trans., 28: 81–101.

Thomas, M.E. and Nordstrom, R.J., 1982b. The N_2-broadened water vapor absorption line shape and infrared continuum absorption — II. Implementation of the line shape. J. Quant. Spectrosc. Rad. Trans., 28: 103–112.

Thomas, M.E. and Nordstrom, R.J., 1985. Line shape model for describing infrared absorption by water vapor. Appl. Opt., 24: 3526–3530.

Varanasi, P., 1988a. Infrared absorptiom by water vapor in the atmospheric window. Proc. Soc. Photo-Instrum. Eng., 928: 213–230.

Varanasi, P., 1988b. On the nature of the infrared spectrum of water vapor between 8 and 14 μm. J. Quant. Spectrosc. Rad. Trans., 40: 169–175.

Submission of manuscripts. Manuscripts in the area of physics of clouds and precipitation should be submitted in triplicate to Dr. J. Dessens.
Manuscripts in the area of atmospheric aerosols, atmospheric chemistry and climate modification should be submitted in triplicate to Dr. A.W. Hogan.
Manuscripts in the area of mesoscale dynamics, remote sensing in the troposphere, instrumentation and observation methods should be submitted in triplicate to Prof. J. Snow.
The indication of a fax and e-mail number on submission of the manuscript could assist in speeding communications. The fax number for the Amsterdam office is +31-20-4852696.
Submission of an article is understood to imply that the article is original and unpublished and is not being considered for publication elsewhere.

Publication information
Atmospheric Research (ISSN 0169-8095). For 1995 volumes 35–38 are scheduled for publication. Subscription prices are available upon request from the publisher. Subscriptions are accepted on a prepaid basis only and are entered on a calendar year basis. Issues are sent by surface mail except to the following countries where air delivery via SAL is ensured: Argentina, Australia, Brazil, Canada, Hong Kong, India, Israel, Japan, Malaysia, Mexico, New Zealand, Pakistan, PR China, Singapore, South Africa, South Korea, Taiwan, Thailand, USA. For all other countries airmail rates are available upon request. Claims for missing issues must be made within six months of our publication (mailing) date. Please address all your requests regarding orders and subscription queries to: Elsevier Science, Journal Department, P.O. Box 211, 1000 AE Amsterdam, The Netherlands. Tel.: +31-20-4853642, fax: +31-20-4853598.

THIS JOURNAL HAS NO PAGE CHARGES

Advertising information
Advertising orders and enquiries may be sent to: Elsevier Science B.V., Advertising Department, P.O. Box 211, 1000 AE Amsterdam, The Netherlands, tel.: +31-20-4853796, fax: +31-20-4853810. Courier shipments to street adress: Molenwerf 1, 1014 PG Amsterdam, The Netherlands. *In the UK*: TG Scott & Son Ltd., attn. Vanessa Bird, Portland House, 21 Narborough Road, Cosby, Leicestershire, LE9 5TA, UK, tel.: 0116-2750521/2753333, fax: 0116-2750522. *In the USA and Canada*: Weston Media Associates, attn. Daniel Lipner, P.O. Box 1110, Greens Farms, CT 06436-1110, USA, tel.: 23-2612500, fax: 23-2610101.

Note to Contributors

A detailed Guide for Authors is available upon request. Please pay attention to the following notes:

Language
The official language of the journal is English, but occasional articles in French and German will be considered for publication.

Preparation of the text
(a) The manuscript should preferably be prepared on a word processor and printed with double spacing and wide margins and include an abstract of not more than 500 words.
(b) Authors should use IUGS terminology. The use of S.I. units is also recommended.
(c) The title page should include the name(s) of the author(s), their affiliations, fax and e-mail numbers. In case of more than one author, please indicate to whom the correspondence should be addressed.

References
(a) References in the text consist of the surname of the author(s), followed by the year of publication in parentheses. All references cited in the text should be given in the reference list and vice versa.
(b) The reference list should be in alphabetical order.

Tables
Tables should be compiled on separate sheets and should be numbered according to their sequence in the text. Tables can also be sent as glossy prints to avoid errors in typesetting.

Illustrations
(a) All illustrations should be numbered consecutively and referred to in the text.
(b) Colour figures can be accepted providing the reproduction costs are met by the author. Please consult the publisher for further information.

Page *proofs*
One set of page proofs will be sent to the corresponding author, to be checked for typesetting/editing. The author is not expected to make changes or corrections that constitute departures from the article in its accepted form. Proofs should be returned within 3 days.

Reprints
Fifty reprints of each article are supplied free of charge. Additional reprints can be ordered on a reprint order form which will be sent to the corresponding author upon receipt of the accepted article by the publisher.